

| | |
|--|---|
| Effects of experimental CO ₂ enrichment on the PSII photochemical | 1 |
| efficiency of <i>Symbiodinium</i> sp. in <i>Acropora millepora</i> | 2 |
| Ashleigh McNie, Daniel Breen, Kay Vopel * | 3 |
| Department of Environmental Science, School of Science, Auckland University of Technology, | 4 |
| Auckland, New Zealand | 5 |
| * Corresponding author | 6 |
| E-mail: kay.vopel@aut.ac.nz | 7 |
| | 8 |

Abstract

9

Enrichment of seawater with CO₂ decreases the concentration of the carbonate ion while increasing that of hydrogen and bicarbonate ions. We use pulse-amplitude-modulation (PAM) fluorometry to investigate whether, in the absence of warming, and in sub-saturating light, these changes affect the PSII photochemical efficiency of *Symbiodinium* sp. in the reef-building coral *Acropora millepora*. We assessed this experimentally with 30-min-interval saturation pulse analyses at 25 °C, a daily peak in the intensity of the photosynthetically active radiation (PAR) at ~65 μmol quanta m⁻² s⁻¹, and a seawater pCO₂ that we gradually increased over nine days from ~496 to ~1290 μatm by injection of CO₂-enriched air. Nine 14-day time series, which, except one, were recorded at the growing apices of a coral branch, revealed diel oscillations in the PSII photochemical efficiency characterized by a steep nocturnal decrease followed by a steep increase and peak in the morning, a daily minimum at midday ($\Delta F/F_m'$,_{midday}), and a daily maximum at the onset of darkness at 19:00 h ($F_v/F_{m,19:00\text{ h}}$). An inadvertent shift in the position of one of the PAM fluorometer measuring heads revealed differences between the basal part and the growing coral apices of a coral branch in $\Delta F/F_m'$,_{midday} and Q_m . In ambient seawater (Control) *Symbiodinium* sp. exhibited a gradual decrease, over the course of the experiment, in $\Delta F/F_m'$,_{midday}, $F_v/F_{m,19:00\text{ h}}$, and the slope of the linear regression between the relative electron transport rate and the intensity of PAR (rETR/PAR). Although two of three successive experiments indicated that CO₂ enrichment counteracted these trends, statistical analyses failed to confirm an influence of pCO₂ on $\Delta F/F_m'$,_{midday}, $F_v/F_{m,19:00\text{ h}}$, and Q_m , rendering this experiment inconclusive.

Keywords

30

CO₂ enrichment; PAM fluorometry; photophysiology; reef-building coral; ocean acidification

31
32

Introduction 33

Enrichment of seawater with CO₂ decreases the concentration of the carbonate ion while 34
increasing that of hydrogen and bicarbonate ions [1]. This shift in the seawater carbonate 35
system occurs in conjunction with ocean warming and can affect coral calcification and 36
photosynthesis, which are intimately coupled [2]. Past experiments have revealed that the 37
coral symbiosis is more susceptible to thermal stress than CO₂ enrichment, and that the 38
physiological plasticity which influences its resilience is species-specific [3–7]. One 39
physiological process of particular interest is the upregulation of the calcifying fluid pH [8,9]. 40
A CO₂ induced increase in seawater [H⁺] may increase the energy required for this 41
upregulation [10] and if so, then such additional energy demand must be compensated by 42
photosynthesis of the symbiotic dinoflagellates, which provide most of the coral's energy by 43
transferring photosynthetic products to their hosts [11]. 44

Coral species apparently differ in their photosynthetic response to CO₂ enrichment due to a 45
host-specific regulation of the symbionts' carbon concentrating mechanism (CCM) [12,13]. 46
The CCM uses active bicarbonate transport and carbonic anhydrase to increase the 47
concentration of CO₂ at the site of type II RuBisCO—an enzyme with a low affinity for CO₂ 48
(14–18]. A high carbonic anhydrase activity may indicate that the coral symbiont lives in a 49
carbon-scarce environment and therefore invests energy in concentrating carbon [13]. In 50
Porites porites (Pallas, 1766) and *Acropora* sp., enrichment of their environment with CO₂ 51
may then increase the gain from photosynthesis for the benefit of the holobiont [19]. 52

In *Acropora muricata* (Linnaeus, 1758), for example, under conditions of sub-saturating light, 53
CO₂ enrichment can increase chlorophyll pigments and the de-epoxidation of xanthophylls, 54
thus increasing the capacity of the symbiont to photoacclimate to low irradiance [20]. The 55
species *Stylophora pistillata* Esper, 1797 responded similarly with an increase in the 56
concentration of chlorophyll pigments and a corresponding increase in photosynthetic 57

efficiency [21], and the symbionts in *A. millepora* (Ehrenberg, 1834) and *Seriatopora hystrix* Dana, 1846 apparently increase their maximum PSII quantum yields and light-limited electron transport rates in response to CO₂ enrichment [22].

Other studies support the view that corals do not respond to CO₂ enrichment [23–26], and yet others have demonstrated negative effects. Kaniewska et al. [27], for example, suggested that in *A. millepora*, CO₂ enrichment caused widespread changes in gene expression consistent with metabolic suppression, an increase in oxidative stress, apoptosis and symbiont loss, and a decrease in respiration and photosynthesis. Furthermore, Edmunds [28] reported negative effects of CO₂ enrichment—in this study, CO₂ enrichment decreased both the symbiont’s maximum and effective photochemical efficiencies.

Here, we follow the studies by Edmunds [28], Hoadley et al. [25], and Noonan and Fabricus [22], asking if, in the absence of warming, CO₂ enrichment affects the PSII photochemical efficiency of *Symbiodinium* sp. in the reef-building coral *A. millepora*. To investigate this experimentally, we conducted time series of saturation pulse analyses (pulse-amplitude-modulation fluorometry) monitoring the symbiont’s maximum photochemical efficiency, F_v/F_m , midday effective photochemical efficiency, $\Delta F/F_m'$, and the relationship between the relative electron transport rate and the intensity of the photosynthetically active radiation (rETR/PAR) while gradually increasing the seawater $p\text{CO}_2$.

Material and methods

Experimental design

We conducted three consecutive laboratory experiments in each of which we acclimated one fragment (~7 cm tall, 4 cm wide) of the coral *A. millepora* for seven days in each of three seawater recirculation tanks to a simulated daily light cycle that peaked midday at a photosynthetically active radiation (hereafter, PAR) of ~65 $\mu\text{mol quanta m}^{-2} \text{ s}^{-1}$ (Fig 1, S1 Fig

1). The nine coral fragments originated from one large *A. millepora* specimen collected off the East Coast of Australia, and therefore, we assume that they hosted the same *Symbiodinium* clade.

After their collection, and until acclimation in the laboratory, the coral fragments were kept under a constant 12/12 h dark/light regime (PAR ~ 90 $\mu\text{mol quanta m}^{-2} \text{s}^{-1}$, Kessil A160WE Tuna Blue LED). In the laboratory, they were placed on a gridded plate under the measuring head of a pulse-amplitude-modulation (PAM) fluorometer (Monitoring-PAM aquatic version, Walz GmbH, Germany) and a Kessil A80 Tuna Blue controllable LED (S1 Figs 1, 2). Because only three PAM fluorometer measuring heads were available for this study, three sets of three time-series measurements were conducted consecutively. For a recent review of the strengths and limitations of chlorophyll fluorescence measurement, see Bhagooli et al. [29].

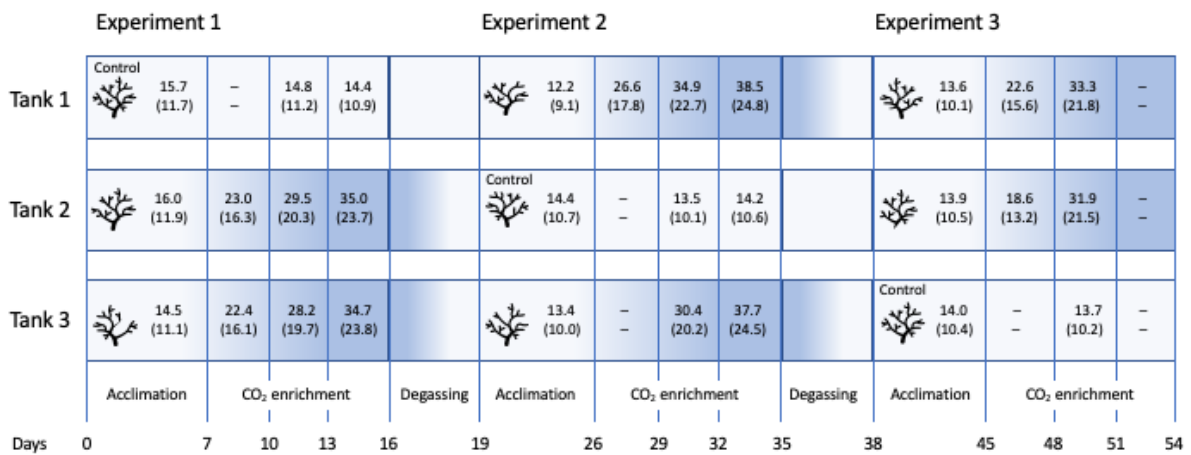


Fig 1. Experimental design and timeline. In each of three consecutive 16-day experiments, one coral fragment was tested in each of three tanks. Transitions from white to blue shades indicate an increase in seawater $p\text{CO}_2$. Numbers, seawater $[\text{CO}_2]$ at 25 °C ($\mu\text{mol kg}^{-1}$); numbers in parentheses, seawater $[\text{H}^+]$ at 25 °C (nmol L^{-1}). N-dashes indicate missing data.

Following 7 days of acclimation, the seawater $p\text{CO}_2$ was gradually raised and then maintained in two of the three tanks from ~500 to ~1200 μatm by computer-controlled injection of CO_2 -

enriched air over the next nine days in three steps. Computer feedback control adjusted CO₂ additions to target pH values, and the three steps resulted in pH = 7.8 on day 10, pH = 7.7 on day 13, and pH = 7.6 on day 16. In each experiment, one of the three tanks remained at ambient pH = 8.0 (Control). Once the first experiment was completed, the CO₂ injection was shut off, allowing the *p*CO₂ in seawater and atmosphere to equilibrate before starting the next experiment on day 19 with three new coral fragments. These steps were repeated before starting Experiment 3 on day 38 (Fig 1).

Laboratory setup

Each experimental tank (S1 Fig 1) contained ~450 L seawater collected from Okahu Bay, New Zealand. A submerged pump (1260, Eheim) moved ~9 L min⁻¹ from the main tank (112 × 72 × 60 cm) through a water cooler (HC-300A, Hailea) and UV sterilizer (Pond One UV-C 9W, ClearTec) into an elevated mixing barrel (210 L) from which the seawater returned to the main tank by gravity. The sizes of the tank and mixing barrel, and the flow rate of the pump, were chosen to ensure that short-term fluctuations in the *p*CO₂ of the seawater in the mixing barrel (due to CO₂ enriched air injection, as explained below) did not affect the tank.

A heater (500 W GH Quartz Glass heater, Aqua One) was placed at the floor of the main tank. The chiller and heater maintained the seawater temperature at 25 ± 0.5 °C. The seawater was also pumped from the main tank through an external particle filter (Professional 4+ 350 Cannister filter, Eheim) into a small, elevated plastic container (30 × 20 × 10 cm) that contained the coral fragment. The tube returning seawater from the particle filter was aimed towards the coral fragment to ensure rapid flow across the coral surface. The overflow from this container returned the seawater into the main tank.

The distance between the measuring head of the PAM fluorometer and the coral surface was ~40 mm. The PAM fluorometer measures ambient light immediately adjacent to the area under test using a small sheet of Teflon placed flush with the measured tissue and reflecting

light to an internal PAR sensor. This sensor was calibrated against a Li-Cor Li-192 underwater quantum sensor. The PAM recordings show that the LED mounted above each coral fragment gradually increased the intensity of PAR from 5 am to a midday maximum of $\sim 65 \mu\text{mol quanta m}^{-2} \text{ s}^{-1}$ and then gradually decreased this intensity until 7 pm, when the LED was turned off (S1 Fig 2). Note that the lowest irradiance emitted from the LED was $\sim 20 \mu\text{mol quanta m}^{-2} \text{ s}^{-1}$. The resulting daily flux, as measured by the internal PAR sensor of the PAM fluorometer, ranged between 1.7 and 2.6 mol quanta $\text{m}^{-2} \text{ day}^{-1}$.

Saturation pulse and induction/recovery analyses

The Walz software WinControl-3.0 ran a batch routine to automatically perform one saturation pulse analysis every 30 minutes between 03:00 and 24:00 h and one daily induction/recovery analyses between 02:00 and 02:30 h. The following settings were applied: saturation pulse intensity = 12, saturation pulse width = 0.6 s, gain = 1, measuring light intensity = 6, measuring light frequency = 3. The measuring light was turned off between saturation pulses and initial measurements of the baseline fluorescence confirmed that the intensity of the measuring light did not cause an actinic light effect. The daily induction/recovery analyses started with an F_0 determination, followed by a series of 12 saturation pulses (delay = 40 s) 20 seconds apart with the actinic light on ($65 \mu\text{mol quanta m}^{-2} \text{ s}^{-1}$). After ~ 4 minutes, the actinic light was turned off, and a series of 8 saturation pulses occurred at increasing intervals between 0.5 and 9 minutes. Prior to deployment, each PAM sensing head was zeroed in the experimental setup.

We derived the maximum PSII photochemical efficiency, F_v/F_m , from measurements of F_0 and F_m in darkness: $F_v/F_m = (F_m - F_0)/F_m$ (Table 1) [30]. The effective photochemical efficiency, $\Delta F/F_m'$, was derived from the maximum (F_m') and minimum (F') fluorescence yields at ambient light intensity: $\Delta F/F_m' = (F_m' - F')/F_m'$ [30]. F_v/F_m measured at 19:00 h, and $\Delta F/F_m'$ measured at midday gave the midday excitation pressure, Q_m : $Q_m = 1 - [(\Delta F/F_m',_{\text{midday}}) /$

($F_v/F_{m,19:00\text{ h}}$) [31]. The PAR recorded by the internal sensor of the PAM and the effective photochemical efficiency, $\Delta F/F_m'$, were used to derive the relative electron transport rate: $rETR = \Delta F/F_m' \times PAR \times 0.5$ [32].

Table 1. Summary of fluorescence parameters measured or derived in conditions of darkness or actinic light. AL, actinic light; SP, saturation pulse.

| Symbol | Fluorescence parameter | Equation/comments | Reference |
|-----------------------------------|------------------------------------|--|-----------|
| Darkness, measured variables | | | |
| F_0 | Minimum fluorescence | | |
| F_m | Maximum fluorescence | Saturation pulse | |
| Darkness, derived variables | | | |
| F_v | Variable fluorescence | $F_v = (F_m - F_0)$ | |
| F_v/F_m | Maximum photochemical efficiency | $F_v/F_m = (F_m - F_0)/F_m$ | [30] |
| Actinic light, measured variables | | | |
| F_m' | Maximum fluorescence yield | Saturation pulse | |
| F_0' | Minimum fluorescence yield | | |
| Actinic light, derived variables | | | |
| F_v' | Variable fluorescence | $F_v' = (F_m' - F_0')$ | |
| $\Delta F/F_m'$ | Effective photochemical efficiency | $\Delta F/F_m' = (F_m' - F_v')/F_m'$ | [30] |
| Q_m | Excitation pressure | $Q_m = 1 - [(\Delta F/F_{m, \text{midday}})/(F_v/F_{m, 19:00\text{ h}})]$ (F_v/F_m measured at 19:00 h, F_m' measured midday) | [31] |
| rETR | Relative electron transport rate | $rETR = \Delta F/F_m' \times PAR \times 0.5$ | [54] |

Seawater carbonate system 156

The pH of the seawater in the mixing barrel of each circulation unit was continuously measured with a SenTix HWD electrode connected to a pH 3310 meter (WTW). These measurements were sent to a computer with CapCtr software (Loligo® Systems ApS) controlling the opening and closing of a solenoid valve when the seawater pH increased above or decreased below the daily set point. The solenoid valve released CO₂-enriched air (5% CO₂, 21% O₂ in nitrogen) from a gas cylinder to a perforated tube in the mixing barrel. The pH electrodes were calibrated using NIST/DIN pH buffers to test for theoretical Nernstian electrode behavior and then conditioned in seawater before determining the electrode-specific offset between the potential measured in NIST/DIN pH buffer and that measured in certified 157
158
159
160
161
162
163
164
165

seawater reference material (TRIS in synthetic seawater). The electrodes were recalibrated at 166
the start of each experiment. 167

Determination of seawater DIC, TA and salinity 168

To determine the seawater carbonate system, we collected a one-liter sample from each 169
circulation unit at the start of each experiment, each night before CO₂-enriched air injection 170
was increased, and at the end of the experiment. These samples were preserved with mercuric 171
chloride and later analyzed for dissolved inorganic carbon (DIC) with a SOMMA (Single 172
Operator Multiparameter Metabolic Analyzer) coulometer system and for total alkalinity (TA) 173
with a closed-cell potentiometric titration system following the SOP's 2 and 3a procedures 174
[33]. We used these DIC and TA measurements and D. Pierrot's adaptation of the 175
CO2Sys.BAS program [34] to compute the seawater *p*CO₂ and pH (total scale, mol kg-SW⁻¹). 176
The dissociation constant for HSO₄⁻ was taken from Dickson [35]; the values of K1 and K2 of 177
carbonic acid were from Mehrbach et al. [36] refitted by Dickson and Millero [37]. Note that 178
water samples were not collected on the final day of Experiment 3 due to a COVID-19 179
pandemic lockdown, and four seawater samples were destroyed during transport to the 180
analytical lab (missing data in Fig 1 and S1 Table 2). The seawater salinity was measured with 181
a handheld conductivity meter (Knick, Germany) and maintained at 34.5 ± 0.5 by daily 182
addition of ultrapure water. 183

Statistical analysis 184

Although saturation pulse analyses were conducted every 30 minutes, we only used the data 185
collected during the last day of each step-*p*CO₂ increase (days 7, 10, 13, 16), considering that 186
during this day, conditions in the experimental tanks had been fully established as per the pH 187
set point. 188

The daily induction/recovery routines were used to assess the effects of CO₂ enrichment on the PSII efficiency using two variables: the variable fluorescence, F_v , determined by analysis of the first saturation pulse of the induction, and the average of the plateaued F_v measured during recovery.

All statistical analyses were performed with R statistical software (version 1.3.959). The Shapiro-Wilk test was used to assess if the data were normally distributed, and homogeneity of variance was tested with the Levenes test. The $F_v/F_{m,19:00\text{ h}}$, $\Delta F/F_{m',\text{midday}}$, Q_m , and the slope of the linear regression of rETR versus incident PAR were analyzed with a four-factor, nested ANOVA in which individual coral fragments were the random factor nested in tank, treatment, and day of measurement, which were fixed factors. The same ANOVAs were then used to analyze the variables derived from the induction and recovery analyses. We used an Akaike information criterion model selection to determine the best model possible to describe the relationship between the fluorescence parameters, the three tanks, the treatment, and the individual coral fragment. The tank effect was not significant and was removed from the model.

Results

Seawater CO₂ enrichment

The measured and derived seawater carbonate chemistry parameters at the start of each of three consecutive CO₂ enrichment experiments (days 7, 26, and 45; Fig 1) and 3, 6, and 9 days later are summarized in Figure 1 and S1 Table 2. The CO2Sys.BAS computations confirmed that the stepwise increase in the injection of CO₂-enriched air increased the $p\text{CO}_2$ of the ambient seawater in the tanks of the Treatments from $493 \pm 44 \mu\text{atm}$ ($n = 6$) to $799 \pm 101 \mu\text{atm}$ ($n = 5$, days 10, 29, and 48), $1109 \pm 89 \mu\text{atm}$ ($n = 6$, days 13, 32, and 51), and $1290 \pm 69 \mu\text{atm}$ ($n = 4$, days 16, 35, and 54; S1 Table 2).

Saturation pulse analyses

213

Time series of saturation pulse analyses revealed diel oscillations in the PSII photochemical

214

efficiency of *Symbiodinium* sp. characterized by a steep nocturnal decrease followed by a

215

steep increase and peak in the morning, a daily minimum at midday, and a daily maximum at

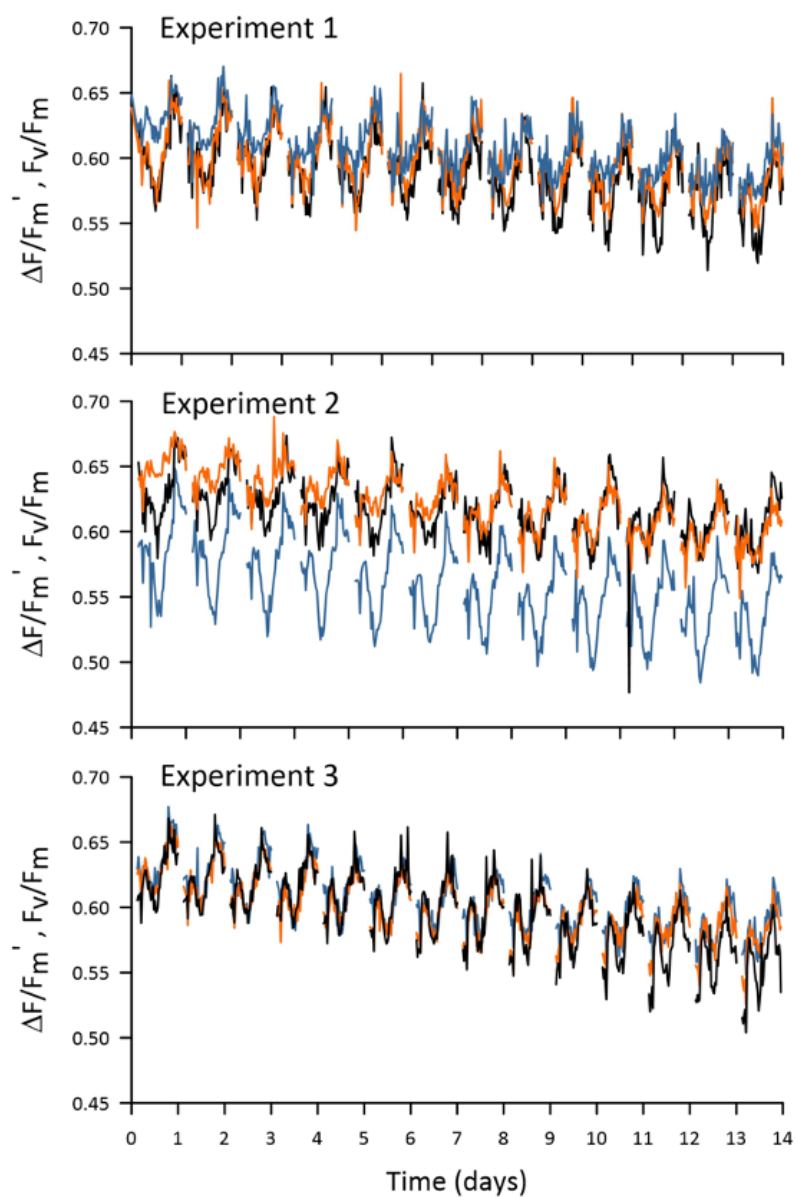
216

the onset of darkness at 19:00 h (Fig 2, S1 Fig 3). We note that the F_v/F_m times series in Fig 2

217

and S1 Fig 3 were interrupted at 02:00 h by photosynthesis induction routines.

218



219

Fig 2. *Symbiodinium* sp. in *Acropora millepora*. Diel variations in the PSII photochemical

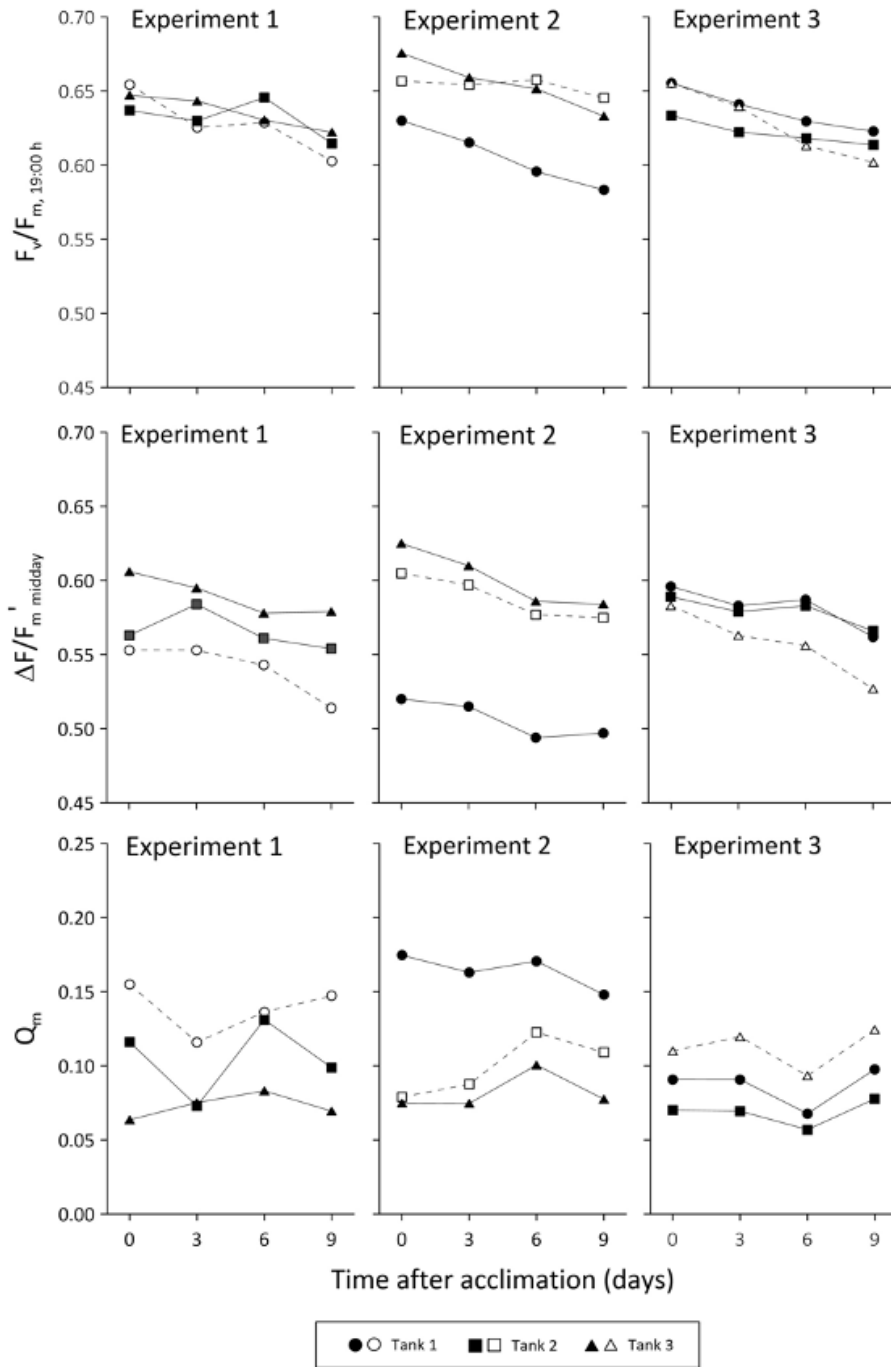
220

efficiency (darkness: F_v/F_m ; light: $\Delta F/F_m'$, see Table 1) of nine coral fragments, one

221

placed in each of three tanks (tank 1, blue; tank 2, black; tank 3, orange) for each of 222
three consecutive experiments. Daily induction and recovery analyses caused gaps in 223
time series from midnight to 03:00 h. 224

Both variables, the maximum PSII photochemical efficiency ($F_v/F_{m,19:00\text{ h}}$ recorded at 19:00 h, 225
Table 1) and the midday effective PSII photochemical efficiency, $\Delta F/F_{m',\text{midday}}$, gradually 226
decreased over the course of the experiment in both Controls and Treatments (Fig 3). This 227
decrease, which produced a significant effect on days 13 and 16 (S1 Table 1), was 228
independent of CO₂ enrichment. Similarly, the midday excitation pressure, Q_m , which was 229
derived from $F_v/F_{m,19:00\text{ h}}$ and $\Delta F/F_{m',\text{midday}}$ (Table 1), was not affected by CO₂ enrichment (Fig 230
3, S1 Table 1). 231



232

Fig 3. *Symbiodinium* sp. in *Acropora millepora*. Time series of the maximum PSII

233

photochemical efficiency measured at 19:00 h, $F_v/F_{m,19:00\text{ h}}$, the midday PSII effective

234

photochemical efficiency, $\Delta F/F_{m',\text{midday}}$, and the midday excitation pressure, Q_m (see

235

Table 1), of nine coral fragments, one placed in each of three seawater circulation units

236

(circles, Tank 1; squares, Tank 2; triangles, Tank 3) in each of three consecutive

237

experiments. In each experiment, the seawater in two tanks (filled symbols) was

238

gradually enriched with CO₂ (Treatment). The pCO₂ in the third unit (open symbols) 239

remained at ~506 μatm over the duration of the experiment (Control). 240

Our measurements on the coral fragment in Tank 1 of Experiment 2 (Treatment, Fig 1) 241

differed from all other measurements in that the PAM measuring head accidentally changed its 242

position so that it was not directed toward the distal but a more basal part of a coral branch. 243

This apparently resulted in much lower PSII photochemical efficiencies (Fig 3). Because the 244

difference in ΔF/F_m'_{midday} was greater than that in F_v/F_m,19:00 h, the derived Q_m exceeded that 245

of the other two coral fragments tested in Experiment 2 (Fig 3). 246

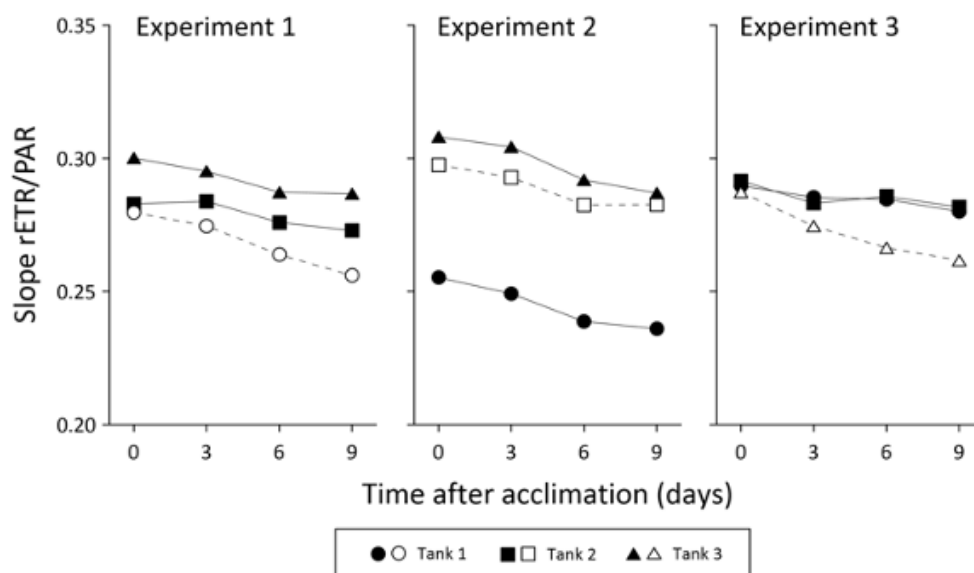
The slope of the linear regression between rETR and PAR (R² > 0.997, S1 Fig 4) decreased 247

over the course of the experiment under ambient pCO₂ conditions (Fig 4, open symbols). 248

Such decrease was also observed in CO₂-enriched seawater (Fig 4, closed symbols), but in 249

Experiments 1 and 3, this decrease was less steep so that the difference in slope between the 250

Control and Treatments increased over the course of the experiment. 251



252

Fig 4. *Symbiodinium* sp. in *Acropora millepora*. Time-series of the slope of the linear 253

regression of relative electron transport rate (rETR) versus incident photosynthetically 254

active radiation (PAR, μmol quanta m⁻² s⁻¹) shown in S1 Fig 4. The rETR was derived 255

from measurements immediately after (day 0) and three, six and nine days after 256
acclimation of nine coral fragments, one placed in each of three seawater tanks (circles, 257
tank 1; squares, tank 2; triangles, tank 3) for each of three consecutive experiments. In 258
each experiment, the seawater in two tanks (filled symbols) was gradually enriched with 259
CO₂ (Treatment, see text and S1 Table 2). 260

Induction–recovery dynamics 261

Like $F_v/F_{m,19:00\text{ h}}$ and $\Delta F/F_m'$,_{midday}, the variable fluorescence, F_v , recorded during the 262
induction–recovery routine decreased over the course of the experiment in both the Control 263
and Treatment groups (S1 Table 3). F_v measured at the beginning of each nocturnal 264
photosynthesis induction was not affected by CO₂ enrichment (S1 Table 3, S1 Fig 5). Once 265
the actinic light was switched off, F_v gradually recovered, approaching pre-light exposure 266
values (F_v between 600 and 800) within 40 min (S1 Fig 5). Again, CO₂ enrichment did not 267
affect the average postinduction recovery F_v (S1 Table 3, S1 Fig 5). 268

Discussion 269

We observed that in ambient seawater (Control) under conditions of a sub-saturating diel light 270
cycle and ~25 °C, *Symbiodinium* sp. exhibited a gradual decrease, over the course of the 271
experiment, in the midday and maximum PSII photochemical efficiency ($\Delta F/F_m'$,_{midday} and 272
 $F_v/F_{m,19:00\text{ h}}$), and the slope of the linear regression between the relative electron transport rate 273
and the intensity of PAR (rETR/PAR). Although two of three successive experiments 274
indicated that CO₂ enrichment counteracted these trends, statistical analyses failed to confirm 275
an influence of $p\text{CO}_2$ on $\Delta F/F_m'$,_{midday}, $F_v/F_{m,19:00\text{ h}}$, and the midday excitation pressure, Q_m , 276
rendering this experiment inconclusive. 277

The midday excitation pressure, Q_m , is an indicator of symbiont performance at maximal 278
irradiance [31]. The near-zero values measured in this study suggest a high proportion of open 279

PSII reaction centers and possible light limitation. The plots in Fig 3 demonstrate that one of 280
the three coral fragments tested in Tank 1 of Experiment 2 exhibited relatively low 281
 $\Delta F/F_m'$,_{midday} and a higher Q_m (Fig 3; filled circles). In this case, the measuring head of the 282
PAM fluorometer had inadvertently changed its position at the onset of the time series, so that 283
it pointed towards the basal part instead of the growing coral apices of a coral branch. This 284
basal part may have exhibited greater light scattering than the distal parts, which would 285
explain the low $\Delta F/F_m'$,_{midday} and higher Q_m [38]. This accidental observation emphasizes the 286
importance of accurate placement of the measuring heads for measurement replication. 287

If we exclude these data for that reason, and consider each experiment separately, then it 288
appears that $\Delta F/F_m'$,_{midday} measured in ambient pCO_2 seawater (Control) was lower than that 289
measured in CO_2 -enriched seawater, in each of the three experiments. On the other hand, the 290
midday excitation pressure, Q_m , was higher than that measured in CO_2 -enriched seawater. 291

Similar effects have been reported for *A. muricata* by Crawley et al. [20] and for *P.* 292
damicornis by Jiang et al. [39], showing that CO_2 enrichment can decrease the PSII excitation 293
pressure. In the former study, this decrease was caused by a reduction in F_v/F_m , while in the 294
latter $\Delta F/F_m'$ increased, as observed in our study. 295

We also note that in Experiments 1 and 3, the slope of the $\Delta F/F_m'$,_{midday} and F_v/F_m ,_{19:00 h} time 296
series measured in increasingly CO_2 enriched seawater was smaller than that of the time series 297
measured in ambient pCO_2 seawater (Fig 3). Similarly, the difference in the slope of the 298
rETR/PAR relationship between Treatments and Control increased as the pCO_2 increased (Fig 299
4). This points to a possible positive effect of CO_2 enrichment; the increasing seawater pCO_2 300
may have counteracted the gradual decrease in $\Delta F/F_m'$ and rETR/PAR slope that was observed 301
under ambient pCO_2 conditions. However, it remains unclear why such a trend was not 302
observed in Experiment 2. If the coral fragments were to host different clades of 303

Symbiodinium, then this may explain a difference in response. However, since the fragments 304
used in our experiment came from the same parental coral, this possibility seems unlikely. 305

We observed that under conditions of ambient $p\text{CO}_2$ F_v/F_m ,19:00 h and $\Delta F/F_m'$,midday gradually 306
decreased over time. Possible causes for this include incomplete acclimation to laboratory 307
conditions. Before our experiment, the coral fragments lived in a constant 12/12 h dark/light 308
regime with a PAR of approximately $90 \mu\text{mol quanta m}^{-2} \text{ s}^{-1}$, providing a daily photon flux of 309
around $3.5 \text{ mol quanta m}^{-2} \text{ day}^{-1}$. In our experiment, the PAR intensity was modulated around 310
a midday peak, resulting in a smaller flux of $1.7\text{--}2.6 \text{ mol quanta m}^{-2} \text{ day}^{-1}$. Although the coral 311
A. millepora appears to tolerate low-light conditions [40,41], it seems that acclimation may 312
take up to 20 days [40], which exceeds the acclimation period in our experiment. Seawater 313
 CO_2 enrichment may have supported such acclimation in Experiments 1 and 3 [20], 314
preventing $\Delta F/F_m'$,midday of the coral fragments from decreasing as steeply as in the Control 315
under conditions of ambient $p\text{CO}_2$. 316

The observed diurnal decline in $\Delta F/F_m'$ (Figs 2, S3) correlated with the daily peak in radiation 317
exposure and possibly the development of reversible and photoprotective non-photochemical 318
quenching [42,43]. On the other hand, the sharp decline in F_v/F_m during the night points to 319
chlororespiration, which can create a trans-thylakoid $[\text{H}^+]$ gradient in the dark through cyclic 320
electron transport around PSI, thereby promoting ATP production [44–46]. Chlororespiration 321
requires oxygen and darkness or at least very low light [47]. In our experiment, these 322
conditions were met at 18:30 h when PAR decreased below $\sim 20 \mu\text{mol quanta m}^{-2} \text{ s}^{-1}$ and was 323
shut down at 19:00 h (S1 Fig 2). 324

Chlororespiration can deplete the accessible oxygen in the coral tissue [48,49]. Without an 325
electron acceptor, electrons may have accumulated in the PSII–PSI electron transport chain, 326
reducing the pool of plastoquinones. This will have initiated the transition of light harvesting 327
complexes from PSII to PSI [44], decreasing the absorption cross section available for PSII 328

[50]. At dawn, F_v/F_m increased rapidly (Figs 2, S1 Fig 3) perhaps following the stimulation of PSI, which oxidized the plastoquinone pool and reversed the transition of light harvesting complexes [45]. Although the function of chlororespiration is still debated [44,51,52), its associated reduction of O_2 accumulated during the day may have lowered the risk of reactive oxygen damage to PSII, and the induced state transition may have supported an efficient onset of photosynthesis and O_2 production at the onset of light (44,53].

Conclusion

Our time series of saturation pulse analyses revealed evidence for chlororespiration of *Symbiodinium* sp. in the reef-building coral *A. millepora*. An inadvertent shift in the position of one of the PAM fluorometer measuring heads revealed differences between the basal part and the growing coral apices of a coral branch in $\Delta F/F_m',_{\text{midday}}$ and Q_m —an accidental observation that emphasizes the importance of accurate sensor placement for measurement replication. Although two of three successive experiments indicated that CO_2 enrichment counteracted the gradual decrease in $\Delta F/F_m',_{\text{midday}}$, $F_v/F_m,_{19:00\text{ h}}$, and the slope of the linear rETR/PAR regression, observed in the Control over the course of the experiment, statistical analyses failed to confirm such effect, rendering this experiment inconclusive. We believe that the possibility of such an effect warrants further experimentation.

Acknowledgments

Evan Brown assisted in the laboratory. Kim Currie, NIWA / University of Otago Research Centre for Oceanography, Dunedin, New Zealand, analyzed the seawater total alkalinity and dissolved inorganic carbon content. The constructive comments of Ian Hawes and Robin Hankin improved the clarity of the manuscript.

Author contributions

A.M. and K.V. conceived and performed the experiment and analyzed the data. K.V. wrote the paper with assistance from A.M. and D.B.

Data availability

The datasets are available from the corresponding author on reasonable request.

References

1. Doney SC, Fabry VJ, Feely RA, Kleypas JA. Ocean acidification: The other CO₂ problem. *Ann Rev Mar Sci.* 2009;6(1): 169–192.
2. Jokiel PL. The reef coral two compartment proton flux model: A new approach relating tissue-level physiological processes to gross corallum morphology. *J Exp Mar Biol Ecol.* 2011;409(1–2): 1–12.
3. Anthony KRN, Kline DI, Diaz-Pulido G, Hoegh-Guldberg O. Ocean acidification causes bleaching and productivity loss in coral reef builders. *PNAS.* 2008;105(45): 17442–17446.
4. Cohen AL, Holcomb M. Why corals care about ocean acidification: Uncovering the mechanism. *Oceanography.* 2009;22(4): 118–127.
5. Uthicke S, Fabricius KE. Productivity gains do not compensate for reduced calcification under near-future ocean acidification in the photosynthetic benthic foraminifer species *Marginopora vertebralis*. *Glob Change Biol.* 2012;18: 2781–2791.
6. Cyronak T, Schulz KG, Jokiel PL. The Omega myth: what really drives lower calcification rates in an acidifying ocean. *ICES J Mar Sci.* 2016;73: 558–562.
7. Bove CB, Davies SW, Ries JB, Umbanhowar J, Thomasson BC, Farquhar EB, et al. Global change differentially modulates Caribbean coral physiology. *PLoS ONE.* 2022;17(9): e0273897.
8. McCulloch MT, D’Olivo JP, Falter J, Holcomb M, Trotter JA. Coral calcification in a changing world and the interactive dynamics of pH and DIC upregulation. *Nat Commun.* 2017;8(1): 1–8.

9. Venn AA, Tambutté E, Holcomb M, Laurent J, Allemand D, Tambutté S. Impact of seawater acidification on pH at the tissue–skeleton interface and calcification in reef corals. *PNAS* 2013;110(5): 1634–1639. 378
379
380
10. Vidal-Dupiol J, Zoccola D, Tambutté E, Grunau C, Cosseau C, Smith KM, et al. Genes regulated to ion-transport and energy production are upregulated in response to CO₂-driven pH decreases in corals: new insights from transcriptome analysis. *PLoS ONE* 2013;8(3): e58652. 381
382
383
384
11. Muscatine L, Falkowski PG, Porter FW, Dubinsky Z. Fate of photosynthetic fixed carbon in light-and shade-adapted colonies of the symbiotic coral *Stylophora pistillata*. *Proc Roy Soc Lond B Biol Sci.* 1984;222(1227): 181–202. 385
386
387
12. Comeau S, Carpenter RC, Edmunds PJ. Coral reef calcifiers buffer their response to ocean acidification using both bicarbonate and carbonate. *Proc Roy Soc Lond B Biol Sci* 2013;280(1753): 20122374. 388
389
390
13. Tansik AL, Fitt WK, Hopkinson BM. Inorganic carbon is scarce for symbionts in scleractinian corals. *Limnol Oceanogr.* 2017;62(5): 2045–2055. 391
392
14. Enns T. Facilitation by carbonic anhydrase of carbon dioxide transport. *Science* 1967;155(3758): 44–47. 393
394
15. Al-Moghrabi S, Goiron C, Allemand D, Speziale N, Jaubert J. Inorganic carbon uptake for photosynthesis by the symbiotic coral-dinoflagellate association II. Mechanisms for bicarbonate uptake. *J Exp Mar Biol Ecol.* 1996;199(2): 227–248. 395
396
397
16. Rowan R, Whitney SM, Fowler A, Yellowlees D. Rubisco in marine symbiotic dinoflagellates: Form II enzymes in eukaryotic oxygenic phototrophs encoded by a nuclear multigene family. *The Plant Cell* 1996;8(3): 539–553. 398
399
400
17. Leggat W, Badger MR, Yellowlees D. Evidence for inorganic carbon-concentrating mechanism in the symbiotic dinoflagellate *Symbiodinium* sp. *Plant Physiol.* 1999;121(4): 1247–1255. 401
402
403
18. Oakley CA, Schmidt GW, Hopkinson BM. Thermal responses of *Symbiodinium* photosynthetic carbon assimilation. *Coral Reefs* 2014;33(2): 501–512. 404
405
19. Herfort L, Thanke B, Taubner I. Bicarbonate stimulation of calcification and photosynthesis in two hermatypic corals. *J Phycol.* 2008;44(1): 91–98. 406
407

20. Crawley A, Kline DI, Dunn S, Anthony KE, Dove S. The effect of ocean acidification on symbiont photorespiration and productivity in *Acropora formosa*. *Glob Change Biol.* 2010;16(2): 851–863. 408
409
410
21. Roberty S, Béraud E, Grover R, Ferrier-Pagès C. Coral productivity is co-limited by bicarbonate and ammonium availability. *Microorganisms* 2020;8(5): 640. 411
412
22. Noonan SH, Fabricius KE. Ocean acidification affects productivity but not the severity of thermal bleaching in some tropical corals. *ICES J Mar Sci.* 2016;73(3): 715–726. 413
414
23. Rodolfo-Metalpa R, Martin S, Ferrier-Pagès C, Gattuso JP. Response of the temperate coral *Cladocora caespitosa* to mid- and long-term exposure to $p\text{CO}_2$ and temperature levels predicted for the year 2100 AD. *Biogeosciences* 2009;7(1): 289–300. 415
416
417
24. Takahashi A, Kurihara H. Ocean acidification does not affect the physiology of the tropical *Acropora digitifera* during a 5-week experiment. *Coral Reefs* 2013;32(1): 305–314. 418
419
420
25. Hoadley KD, Pettay DT, Grottoli AG, Cai WJ, Melman TF, Schoepf V, et al. Physiological response to elevated temperature and $p\text{CO}_2$ varies across four Pacific coral species: Understanding the unique host+symbiont response. *Sci Rep.* 2015;5(1): 1–15. 421
422
423
26. Enochs IC, Derek P, Manzello DP, Carlton R, Schopmeyer S, Van Hooidek R, Lirman D. Effects of light and elevated $p\text{CO}_2$ on the growth and photochemical efficiency of *Acropora cervicornis*. *Coral Reefs* 2014;33(2): 477–485. 424
425
426
27. Kaniewska P, Campbell PR, Kline DI, Rodriguez-Lanetty M, Miller D J, Dove S, Hoegh-Guldberg O. Major cellular and physiological impacts of ocean acidification on a reef building coral. *PLoS ONE* 2012;7(4): e34659. 427
428
429
28. Edmunds PJ. Effect of $p\text{CO}_2$ on the growth, respiration, and photophysiology of massive *Porites* spp. in Moorea, French Polynesia. *Mar Biol.* 2012;159(10): 2149–2160. 430
431
29. Bhagooli R, Mattan-Moorgawa S, Kaullysing D, Louis YD, Gopeechund A, Ramah S et al. Chlorophyll fluorescence – a tool to assess photosynthetic performance and stress photo-physiology in symbiotic marine invertebrates and seaplants. *Mar Pollut Bull.* 2021;165: 112059. 432
433
434
435
30. Kitajima MB, Butler WL. Quenching of chlorophyll fluorescence and primary photochemistry in chloroplasts by dibromothymoquinone. *BBA–Bioenergetics* 1975;376(1): 105–115. 436
437
438

31. Iglesias-Prieto R, Beltrán VH, LaJeunesse TC, Reyes-Bonilla H, Thomé PE. Different algal symbionts explain the vertical distribution of dominant reef corals in the eastern Pacific. *Proc R Soc Lond Ser B*. 2004;271: 1757–1763.
32. Klughammer C, Schreiber U. Complimentary PSII quantum yields calculated from simple fluorescence parameters measured by PAM fluorometry and the saturation pulse method. *PAM Application Notes* 2008;1(2): 201–247.
33. Dickson AG, Sabine CL, Christian JR. Guide to best practices for ocean CO₂ measurements: PICES Special Publication 3. 2007. http://cdiac.ornl.gov/oceans/Handbook_2007.html
34. Lewis E, Wallace DWR. Program developed for CO₂ system calculations. ORNL/CDIAC-105. Carbon Dioxide Information Analysis Center, Oak Ridge National Laboratory, U.S. Department of Energy, Oak Ridge, Tennessee, 1998
35. Dickson AG (). Standard potential of the reaction: $\text{AgCl}_{(s)} + 12\text{H}_2_{(g)} = \text{Ag}_{(s)} + \text{HCL}_{(aq)}$, and the standard acidity constant of the ion HSO_4^- in synthetic seawater from 273.15 to 318.15 K. *J Chem Thermodyn*. 1990;22: 113–127.
36. Mehrbach C, Culberson CH, Hawley JE, Pytkowicz RN. Measurement of the apparent dissociation constants of carbonic acid in seawater at atmospheric pressure. *Limnol Oceanogr*. 1973;18: 897–907.
37. Dickson AG, Millero FJ. A comparison of the equilibrium constants for the dissolution of carbonic acid in seawater media. *Deep Sea Res*. 1987;34(10): 1733–1743.
38. Enriquez S, Méndez ER, Iglesias-Prieto R. Multiple scattering on coral skeletons enhances light absorption by symbiotic algae. *Limnol Oceanogr*. 2005;50: 1025–1032.
39. Jiang L, Guo YJ, Zhang YY, McCook LJ, Yuan XC, Lei XM, et al. Diurnally fluctuating $p\text{CO}_2$ modifies the physiological responses of coral recruits under ocean acidification. *Front Physiol*. 2019;9: 1952.
40. DiPerna S, Hoogenboom M, Noonan S, Fabricius K. Effects of variability in the daily light integrals on the photophysiology of the corals *Pachyseris speciosa* and *Acropora millepora*. *PLoS ONE* 2018;13(9): e0203882.
41. Kuanui P, Chavanich S, Viyakarn V, Omori M, Fujita T, Lin C. Effect of light intensity on survival and photosynthetic efficiency of cultured corals of different ages. *Estuar Coast Shelf Sci*. 2020;235: 106515.

42. Ralph PJ, Gademann R, Larkum AWD, Schreiber U. In situ underwater measurements of photosynthetic activity of coral zooxanthellae and other reef-dwelling dinoflagellate endosymbionts. *Mar Ecol Prog Ser.* 1999;180: 139–147. 470
471
472
43. Gorbunov MY, Kolber ZS, Lesser MP, Falkowski PG. Photosynthesis and photoprotection in symbiotic corals. *Limnol Oceanogr.* 2001;46: 75–85. 473
474
44. Jones RJ, Hoegh-Guldberg O. Diurnal changes in the photochemical efficiency of the symbiotic dinoflagellates (Dinophyceae) of corals: photoprotection, photoinactivation and the relationship to coral bleaching. *Plant Cell Environ.* 2001;24(1): 89–99. 475
476
477
45. Hill R, Ralph PJ. Diel seasonal changes in fluorescence rise kinetics of three scleractinian corals. *Funct Plant Biol.* 2005;32: 549–559. 478
479
46. Rumeau D, Peltier G, Cournac L. Chlororespiration and cyclic electron flow around PSI during photosynthesis and plant stress response. *Plant Cell Environ.* 2007;30(9): 1041–1051. 480
481
482
47. Bennoun P. Chlororespiration revisited: mitochondrial-plastid interactions in *Chlamydomonas*. *BBA–Bioenergetics.* 1994;1186(1–2): 59–66. 483
484
48. Shashar N, Cohen Y, Loya Y. Extreme diel fluctuations of oxygen in diffusive boundary layers surrounding stony corals. *Biol Bull.* 1993;185(3): 455–461. 485
486
49. Kühl M, Cohen Y, Dalsgaard T, Jørgensen BB, Revsbech NP. Microenvironment and photosynthesis of zooxanthellae in scleractinian corals studied with microsensors for O₂, pH and light. *Mar Ecol Prog Ser.* 1995;117(1–3): 159–172. 487
488
489
50. Warner ME, Berry-Lowe S. Differential xanthophyll cycling and photochemical activity in symbiotic dinoflagellates in multiple locations of three species of Caribbean coral. *J Exp Mar Biol Ecol.* 2006;339(1): 86–95. 490
491
492
51. Nixon PJ. Chlororespiration. *Philos Trans R Soc Lond B: Biol Sci.* 2000;355(1402): 1541–1547. 493
494
52. Hill R, Ralph PJ. Dark-induced reduction of the plastoquinone pool in zooxanthellae of scleractinian corals and implications for measurements of chlorophyll a fluorescence. *Symbiosis* 2008;46(1): 45–56. 495
496
497
53. Norrick WJ, Buchert F, Joliot P, Rappaport F, Bailleul B, Wollman FA. Chlororespiration controls growth under intermittent light. *Plant Physiol.* 2019;179(2): 630–639. 498
499

54. Schreiber U, Endo T, Mi H, Asada K. Quenching analysis of chlorophyll fluorescence by the saturation pulse method: Particular aspects relating to the study of eukaryotic algae and cyanobacteria. *Plant and Cell Physiology* 1995;36(5): 873–882.